SLAC-PUB-3027
ANL-HEP-8302
December 1982
M

HIGHER TWIST CONTRIBUTIONS TO LEPTON-PAIR PRODUCTION AND OTHER QCD PROCESSES*

STANLEY J. BRODSKY
Stanford Linear Accelerator Center
Stanford University, Stanford, California 94305

and

EDMOND L. BERGER
High Energy Physics Division
Argonne National Laboratory, Argonne, Illinois 60439

and

G. PETER LEPAGE
Laboratory of Nuclear Studies
Cornell University, Ithaca, New York 14853

ABSTRACT

A general discussion of the calculations and phenomenological consequences of power-law suppressed QCD processes is given with emphasis on tests in massive lepton pair production. Absolutely normalized predictions are given for the leading twist (transverse current) and higher twist (longitudinal current) contributions to the meson structure function in the region of large x.

---

* Work supported by the Department of Energy, contract DE-AC03-76SF00515.

(Presented by S.J.B. at the Workshop on Drell-Yan Processes, Fermilab, Illinois, October 7-8, 1982.)

1. INTRODUCTION

One of the most serious complications in testing quantum chromodynamics is the presence of power-law suppressed contributions.[1] There are numerous dynamical and kinematical sources of such terms: finite mass corrections, transverse momentum smearing effects, resonance contributions, low relative velocity threshold effects, endpoint integration region corrections, contributions from initial and final state interactions among the active and spectator constituents, multiple-scattering processes[2] [see Fig. 1(a)], pinch singularities, interference contributions from different subprocesses [see Fig. 1(b)], higher-particle number subprocesses such as "direct" meson reactions[3] and exclusive channel contributions. In some cases, such as deep inelastic scattering, the power-law terms directly correspond to higher twist contributions in the operator product expansion.[1,4] In addition there are power-law suppressed nonperturbative contributions unique to non-Abelian theory from vacuum fluctuations (instantons)[5] and effects related to confinement and jet fragmentation.

Empirically, the power-law suppressed contributions can camouflage the logarithmic scale-violating behavior predicted by QCD for the leading twist contributions. This is a particularly serious problem in the analysis of deep inelastic structure functions at moderate Q^2.[6] One of the reasons the value of the scale constant Λ_s of QCD is so difficult to determine unambiguously is that the kinematic region most sensitive to the parameterization of $\alpha_s(Q^2)$ is the same region where the higher twist terms are large. In some cases, higher twist contributions can actually dominate the leading twist contributions. For example, meson structure functions and fragmentation functions near the $x \sim 1$ kinematic limit are predicted in perturbative QCD to have the nominal behavior (ignoring logarithmic corrections)[7,8]

$$F_2^M(x,Q) \underset{x\to 1}{\sim} A\left[(1-x)^2 + \frac{\lambda^2}{Q^2}\right] \tag{1.1}$$

where the scale λ is set by the hadronic wave function. Thus the higher twist term can dominate for

$$(1-x) \leq \frac{\lambda}{Q} . \tag{1.2}$$

In the case of single particle hadron production at large transverse momentum in hadron collisions, "higher twist" direct processes such as $gq \to Mq$ [9] can dominate the usual hard scattering process contributions $qq \to qq$, $gq \to gq$ etc. at moderate p_T because of the "trigger bias" suppression against processes requiring jet fragmentation. Such power-suppressed terms may help to account for the power-law scaling behavior observed for $p_T \leq 8 GeV/c$ in the FNAL-ISR energy regime $[d\sigma/d^3p/E \sim p_T^{-8} f(x_T, \theta_{c.m.})$ for meson production, $\sim p_T^{-12} f(x_T, \theta_{c.m.})$ for proton production], and the strong charge correlations observed between the trigger particle and away side jet particles.[10]

Although higher twist power-suppressed contributions are usually regarded as unwelcome complications in QCD phenomenology, we will take the view here that such effects should be isolated and studied as novel and interesting probes of hadronic dynamics. Among the coherence effects which can be studied are (1) the multiparticle correlations of the hadronic wave functions, (2) the analytic connections between semi-inclusive and exclusive phenomena, (3) color transparency effects in semi-exclusive reactions, and (4) novel forms of QCD evolution.

In the next sections we will review a convenient calculational framework for higher twist processes and discuss their phenomenological consequences, especially in massive lepton pair production.[11]

2. PERTURBATIVE ANALYSIS

Contributions to inclusive processes which are analyzable in perturbative QCD can be organized in terms of a hard-scattering expansion[12] $d\sigma \sim \sum_n G_n \otimes d\hat{\sigma}_n$ where the overall power-law scaling behavior of each (quasi-on-shell) subprocess cross section $d\hat{\sigma}_n(Q)$ in the momentum transfer Q is controlled by the number of elementary fields experiencing the momentum transfer [see Fig. 2(a)]. The nominal scaling behavior in Q^{-2} is given by the dimensional counting rules. The G_n are probability distributions computed from the hadronic wave functions. Equivalently, one can use the operator product expansion to identify the basic short distance subprocesses; the QCD equations of motion are then used to eliminate derivatives corresponding to $k_\perp$ smearing and off-shell effects in favor of operators which correspond to near on-shell multiparticle scattering processes.[13] A consistent operator basis which can eventually lead to a solution of the operator mixing problem and full QCD evolution structure of leading and power suppressed contributions is given in Ref. 13.

A central question in QCD is the nature of corrections due to nonperturbative effects, whether from hadronic wave functions, fragmentation processes, instantons, or other effects due to the nonperturbative vacuum. The nonperturbative effects could be sufficiently singular to give important power-law suppressed contributions or modify the evolution of higher twist contributions.[14] From a phenomenological point of view, analyses of jet data are strongly dependent on the models used for fragmentation distributions,[15] leading to variations of order $\pm 50\%$ in the magnitude of α_s extracted from $e^+e^- \to 3$ jet events.[16] In addition, as shown by Gupta and Quinn,[17] the standard picture of jet hadronization cannot be correct if all quark masses are large compared to the QCD scale Λ. Thus there must be a hidden analytic dependence on the quark mass beyond what is indicated by perturbation theory.

The general question of nonperturbative effects is thus a central problem for calculating higher twist terms. In this review we will focus on multiparticle scattering contributions whose leading power-law behavior is unaffected by mass and scalar insertions so that perturbation theory could be reliable. In addition, in many cases we will be able to avoid many questions of nonperturbative effects by evaluating the higher twist contribution in terms of measured quantities, such as the meson form factor.

The basic dynamical structure of the required multiparticle scattering amplitudes and their hadronic matrix elements follows immediately from the formalism given in Ref. 18 for exclusive scattering amplitudes. Hadronic matrix elements are given by the convolution of a multiquark/gluon hard scattering subprocess amplitude T_H with the QCD Fock state wave functions of the hadrons $\psi_{(n)}(x^i, \vec{k}^i_\perp)$ defined at equal $\tau = t + z$ on the light-cone. For example, the higher twist subprocess $\gamma + (qq) \rightarrow q + q$ which gives a contribution to the cross section for $\gamma + p \rightarrow Jet + Jet + X$ can be written in the form [see Fig. 2(b); a = active; s = spectator]

$$\begin{aligned} \mathcal{M}_{(n)} = \int^{(k^a_\perp)^2 < Q^2} & \prod_a (d^2 k^a_\perp \, dx^a) \psi^Q_{(n)}(x^a, k^a_\perp; x^s, k^s_\perp) \\ & \times T_H(x^a, Q) \delta(\textstyle\sum x^a - x^A) \delta^2(\textstyle\sum k^a_\perp - k^A_\perp) \end{aligned} \tag{2.1}$$

where $T_H(x^a, Q)$ is the connected hard scattering amplitude for $\gamma + (qq)_A \rightarrow q + q$ computed for the "active" quarks collinear with the incident proton, and $\psi^Q_{(n)}(x^a, k^a_\perp; x^s, k^s_\perp)$ is an n-particle proton Fock state defined at equal τ which contains the two active quarks as well as "spectator" quarks and gluons. By the definition of T_H, the transverse momentum of the active constituents is limited internally in ψ^Q to $k^{a2}_\perp < Q^2$. The contributions from $(k_\perp^a)^2 > Q^2$ are contained in $T_H(x_i^a, Q)$; in fact, since all the virtual legs in T_H are hard, $T_H(x_i^a, Q)$ can be expanded in perturbation theory in powers of $\alpha_s(Q)$. The form (2.1) is of course generalizable to multihadron processes.

The amplitude $\mathcal{M}_{(n)}$ in Eq. (2.1) is dependent on the wave function for finding all the active quarks at impact separation $b_\perp^a \sim O(1/Q)$ and light-cone momentum fractions x^a. The subprocess cross section is then computed by squaring $\mathcal{M}_{(n)}$, integrating over the spectator momenta, and summing over the contributing Fock states $\psi_{(n)}$. The net result for the $\gamma p \to JetX$ cross section is thus a series of the nominal form $[\theta_{c.m.} \sim (\pi/2)$, $x_T = (2p_T/\sqrt{s}) \sim 1]$

$$
\begin{aligned}
\frac{d\sigma}{d^3p/E}(\gamma p \to q + X) \sim & \frac{\alpha\alpha_s(p_T^2)}{p_T^4}(1-x_T)^3 \, , \; (\gamma q \to qg) \\
& + \frac{\alpha\alpha_s^2(p_T^2)\lambda^2}{p_T^6}(1-x_T)^2 \, , \; (\gamma qq \to qq) \\
& + \ldots
\end{aligned}
\qquad (2.2)
$$

where λ^2 is the hadronic scale controlled by the correlation of the active quarks in the wave function. Despite their faster fall-off in p_T, the power suppressed contributions can become important at the edge of phase space $x_T \to 1$, since a large fraction of the incident hadron momentum is carried by the active constituents. Rules for counting the powers of p_T^2 and $(1 - x_T)$ including modifications due to spin mismatch are given in Ref. 19.

3. DIRECT HIGHER TWIST PROCESSES

One of the most interesting examples of higher twist phenomena is the set of "direct" processes in which all of the valence quarks of a hadron participate in the hard scattering process.[3,9,20–22] An example [see Fig. 3(a)] is the subprocess $\pi_D g \to q\bar{q}$ which produces large p_T jets in πp collisions without associated hadron production in the forward fragmentation direction; i.e., the pion's momentum is completely consumed in the hard-scattering reaction. Direct hadron reactions are analogous to direct or prompt photon processes. The entire Fock state at small impact parameter appears in the hard scattering reaction without accompanying collinear hadronic radiation.[23]

The required wave function for calculating a direct hadron subprocess amplitude is the "distribution amplitude"

$$\phi(x^a, Q) \equiv \int^{(k_\perp^a)^2 < Q^2} \prod_a d^2 k_\perp^a \, \delta(\Sigma k_\perp^a) \psi_V^Q(x^a, k_\perp^a) \tag{3.1}$$

where ψ_V is the lowest particle number $|q\bar{q}\rangle$ or $|qqq\rangle$ Fock state amplitude. The distribution amplitude, originally defined for exclusive processes,[18] is the probability amplitude for finding the valence quarks of a hadron at small impact separation $b_\perp^a \sim 1/Q$.

The jet cross section based on the $\pi_D g \to q\bar{q}$ (and $\pi_D q \to gq$) subprocess in Fig. 3 can be absolutely normalized in terms of the pion form factor since the same integral of the pion distribution amplitude appears in each case. Averaging over color the subprocess cross sections are[3]

$$\frac{d\sigma}{dt}(\pi_D q \to gq) = \frac{16}{27} \frac{\pi \alpha_s^2}{s^2} F_\pi(s) \left[-\frac{t}{s} - \frac{ts}{u^2} \right] \tag{3.2}$$

and

$$\frac{d\sigma}{dt}(\pi_D g \to q\bar{q}) = \frac{2}{9} \frac{\pi \alpha_s^2}{s^2} F_\pi(s) \left[\frac{s^2}{u^2} + \frac{s^2}{t^2} \right] \tag{3.3}$$

i.e.,

$$d\sigma(\pi_D p \rightarrow Jet + Jet + X) \propto F_\pi(p_T^2)\, d\sigma(leading\ twist)\,, \tag{3.4}$$

independent (in leading order) of $\alpha_s(p_T^2)$ and the pion wave function.

The direct process thus scales as $(d\sigma/d^3p/E) \sim p_T^{-6} f(x_T, \theta_{c.m.})$. It is experimentally identifiable by conservation of the $p^+ = p^0 + p^3$ components between the pion and jet fragments, and the close transverse momentum balance of the high p_T jets. No spectator jet emerges along the beam axis direction. Observation of the these unique events at the predicted rate is important since it tests the basic principle that a pion has a nonzero probability to exist as a q and $\bar{q}$ Fock amplitude with small transverse separation. In the case of nuclear target reactions, e.g. $\pi_D A \rightarrow q\bar{q}X$, the valence state with $b_\perp \simeq O(1/p_T)$ should penetrate the nuclear volume without elastic or inelastic hadronic interactions. The absence of induced reaction in the nucleus for the direct processes thus tests the idea of "color transparency", i.e., color singlet states of vanishing radius have no strong interactions.[24]

The corresponding direct baryon induced reaction based on the subprocess $\bar{p}_D q \rightarrow \bar{q}\bar{q}$ is shown in Fig. 3(c). The cross section for $\bar{p}_D p \rightarrow Jet + Jet + X$ scales roughly as $F_p(p_T^2)$ times the leading twist cross section and gives a measure of the valence amplitude of the antiproton. Similarly, the amplitude for finding three quarks in the proton at small separation together with a pionic spectator $(q\bar{q})$ system in the Fock state can be measured by an analogous process $\bar{p}_D p \rightarrow \bar{q}\bar{q}\pi X$. The normalization of such higher Fock state components is required to compute the amplitude for baryon decay in grand unified theories.[25]

In the case of hadron production at large p_T, the direct subprocesses $gq \rightarrow \pi_D q$ [see Fig. 4(a)] and $q\bar{q} \rightarrow \pi_D g$ produce pions unaccompanied by other hadrons on the trigger side. These p_T^{-6} QCD processes are again absolutely normalized[9] in terms of the meson form factor, and for certain regions of phase space (moderate p_T, large x_T) can dominate jet fragmentation processes. More generally, an entire set of hadrons and resonances can be produced by the direct subprocesses ($gq \rightarrow M^* q$, $q\bar{q} \rightarrow M^* g$, $qq \rightarrow B^* \bar{q}$, $qB \rightarrow qB^*$, etc) and can constitute a serious background to leading twist single particle cross sections. Since the hadron valence state interacts directly at small constituent separation, the directly produced hadrons have no final state interactions or accompanying collinear radiation to leading order in $1/p_T^2$.

Detailed, absolutely normalized QCD predictions have also been worked out for the direct meson production of high transverse momentum prompt photons[20–22] and lepton pairs[8,21,26] [see Fig. 4(b)], and direct photon production of high transverse momentum prompt mesons.[20–22] In each of these cases the higher twist contribution can be a significant contribution compared to the standard leading twist result and is a useful probe of QCD dynamics.

A similar analysis can be given for direct meson production at large transverse momentum relative to the quark jet axis in $e^+e^- \rightarrow \bar{q}q \rightarrow \bar{q}qM$ [see Fig. 4(c)]. The tail of the meson production distribution is of the form[27]

$$\frac{dN}{dk_\perp^2} \sim \frac{\alpha_s(k_\perp^2)}{k_\perp^2}\ ,\ \frac{\alpha_s(k_\perp^2)}{k_\perp^2} F_M(k_\perp^2) \tag{3.5}$$

from $q\bar{q}g$ jet fragmentation and $q\bar{q}M$ higher twist contributions respectively. The direct meson contribution thus has a $k_\perp^4$ power-law fall-off rather than the Gaussian parameterization usually assumed for $q \rightarrow q + M$ fragmentation. The power-law higher twist background summed over all hadrons and resonances may not be large in magnitude,[21,28] but it could imply that the probability of three jet $e^+e^-\to q\bar{q}g$ leading twist events and thus $\alpha_s(Q^2)$ has been overestimated in standard perturbative analyses.

4. HIGHER TWIST CONTRIBUTIONS TO STRUCTURE FUNCTIONS

An important test of QCD dynamics is the behavior of the quark and gluon distribution functions of hadrons at light-cone fraction $x\sim 1$. The distribution functions can be conveniently defined in terms of the light-cone Fock state wave functions[29]

$$G_{a/H}(x^a, Q) = \sum_n \int^{k_\perp^2<Q^2} \prod_{i\neq a} \left(\frac{d^2k_\perp^i}{2(2\pi)^3} dx^i\right) |\psi_n^Q(x^i, k_\perp^i)|^2 \sum_{j=a} \delta(x^a - x^j) \quad (4.1)$$

integrated over all unobserved momenta and summed over all Fock states. (The $\sum_j$ is over all constituents of type a in the Fock state n.) In the endpoint region $x_a\sim 1$ the wavefunction is evaluated far off-shell:

$$\epsilon_n = \frac{k_a^2 - m_a^2}{x_a} = M^2 - \sum_{i=1}^{n} \left(\frac{k_\perp^2 + m^2}{x}\right)_i \underset{x_a\to 1}{\sim} \frac{-\mu^2}{1-x_a} \quad (4.2)$$

provided $(k_\perp^2 + m^2)_{i\neq a}\sim\mu^2$ is nonzero. It is thus reasonable to compute the leading $x_a\to 1$ behavior from perturbative, hard-gluon exchange diagrams. The nominal power-law behavior computed from the valence Fock state is[30]

$$G_{q/p}(x)\sim\begin{cases}(1-x)^3 & \textit{parallel quark, proton helicities}\\ (1-x)^5 & \textit{antiparallel quark, proton helicities}\end{cases} \quad (4.3)$$

and

$$G_{q/\pi}(x)\sim(1-x)^2 \ . \quad (4.4)$$

The higher Fock states either give QCD evolution corrections (radiation from active quark) or higher power-law fall-off contributions at $x \rightarrow 1$.

One can also identify another contribution[31] to the distribution functions at $x_a \sim 1$ from the soft integration region $(k_\perp^2)_{i \neq a} \leq O(1 - x_a)\mu^2$. Note that in this region ϵ_n is nearly on-shell if the quark mass terms can be neglected. Integration over the phase space of the spectator quarks then gives

$$G_{a/H}(x) \sim (1 - x)^{2n_s - 1} F_H(x) \tag{4.5}$$

where n_s is the number of spectators $i \neq a$ in the valence Fock state. The function $F_H(x)$ presumably gives additional fall-off due to the behavior of the wave function for small spectator momentum, but it is incalculable in perturbation theory. The SLAC-Yale[32] measurements of the quark spin correlation in deep inelastic polarized e-p scattering, however, gives support for the dominance of the perturbative contributions, Eq. (4.3).

The perturbative analyses of structure functions in the endpoint region can be justified in detail using the operator product expansion or from the light-cone perturbation theory formalism used to derive QCD evolution equations for the distribution amplitude.[18] We assume that the nonperturbative wave function falls off rapidly in the endpoint region. For large off-shell energies we can then calculate the valence wave function from the leading behavior of the interaction kernel in the wave function equation of motion. For example, for the meson wave function at $x \sim 1$, $\epsilon_2 \sim -k_\perp^2/(1 - x)$ and to leading order in $\alpha_s(\epsilon_2)$

$$\psi_2(x,k_\perp) = \frac{(1-x)}{k_\perp^2} 8\pi\alpha_s(\epsilon_2) C_F \int_0^x dy \frac{\phi(y,\epsilon_2)}{1-y}\left(1+\frac{1}{x-y}\right)$$
$$+ [x\to(1-x)\,,\ y\to(1-y)] \tag{4.6}$$

where $C_F = 4/3$. Thus for $(x\sim 1)$ we have the (absolutely normalized) contribution to the meson structure function

$$G_{q/M}(x) = (1-x)^2 \int \frac{dk_\perp^2}{k_\perp^4}$$
$$\times \left[\int_0^1 \frac{dy}{1-y}\, 2C_F\alpha_s\left(\frac{k_\perp^2}{1-x}\right)\phi\left(y, \frac{k_\perp^2}{1-x}\right)\cdot\left(1+P\,\frac{1}{(x-y)}\right)\right]^2 \tag{4.7}$$

The infrared divergence at $y\to x$ in the valence wave function (4.6), as defined in the light-cone gauge ($A^+ = 0$), cancels in the meson structure function (4.7) when one includes a corresponding contribution from soft-gluon radiation. In addition, QCD radiative corrections lead to the further logarithmic evolution of $G_{q/M}(x,Q^2)$ at large Q^2.[30,33] Equation (4.7) gives the contribution to the structure function from large off-shell energy $|\epsilon_2| = k_\perp^2/(1-x)$, i.e., $k_\perp^2 > |\epsilon_2|(1-x)$.

Alternatively, we can compute the deep inelastic structure functions of a meson at $x\sim 1$ from the convolution of $\psi_2(y,j_\perp)$ and the $T_H(q\bar{q}+\gamma^*\to q+\bar{q})$ hard scattering amplitude, as in Eq. (2.1) [see Fig. 5(a)].

$$W^{\mu\nu} = \frac{1}{2\pi}\int_0^1 dz \int \frac{d^2\ell_\perp}{2(2\pi)^3} \mathcal{M}^{\mu\dagger}\mathcal{M}^{\nu}\,\pi\delta\left(\frac{Q^2}{x} - \frac{Q^2+2q_\perp\cdot\ell_\perp}{z} - \frac{\ell_\perp^2}{z(1-z)}\right) \tag{4.8}$$

where

$$\mathcal{M}^{\mu}_{\gamma*\to q\bar{q}} = \int_0^1 dy\, \phi\left(y, \frac{\ell_\perp^2}{1-z}\right) T^{\mu}_{\gamma* q\bar{q}\to q\bar{q}}\,. \tag{4.9}$$

We have chosen the frame ($p^{\pm} = p^0 \pm p^3$)

$$\begin{aligned} p_\pi &= (p^+, p^-, p_\perp) = \left(p^+, \frac{M^2}{p^+}, \vec{O}_\perp\right) \\ q &= (q^+, q^-, q_\perp) = \left(0, \frac{2p\cdot q}{p^+}, q_\perp\right) \end{aligned} \tag{4.10}$$

with $-q^2 = Q^2 = q_\perp^2$, $x = Q^2/2p\cdot q$, and $z = \ell^+/p^+$. To leading order in $\alpha_s(\ell_\perp^2/(1-z))$ the important region of integration in the wave function is $j_\perp^2/(y(1-y)) \ll \ell_\perp^2/(z(1-z))$, which together with wavefunction renormalization, is absorbed into the meson distribution amplitude. In addition, to this order $T_{\gamma* q\bar{q}\to q\bar{q}}$ can be computed from the lowest order tree graphs with the incident q and $\bar{q}$ collinear with p_π.[26]

The leading behavior of the meson structure functions can then be computed from $W^{++} = (p^+p^+/p\cdot q)F_2$, $W^{--} = (Q^2/x^2p^+p^+)F_L$, and $F_2 = 2x(F_1 + F_L)$. We obtain ($x \sim 1$)

$$F_2^M(x, Q^2) = \sum_q e_q^2\, x\, G_{q/M}(x) \tag{4.11}$$

where $G_{q/M}$ is again given by (4.7) and[34] $[W^2 = (1-x)Q^2/x]$

$$
\begin{aligned}
F_L^M(x,Q^2) &= \sum_q 2e_q^2 \frac{x^2}{Q^2}\int_{\mu^2}^{W^2} \frac{d\ell_\perp^2}{\ell_\perp^2}\left[\int_0^1 \frac{dy}{1-y} 2C_F\alpha_s\left(\frac{\ell_\perp^2}{1-x}\right)\phi\left(y,\frac{\ell_\perp^2}{1-x}\right)\right]^2 \\
&= \sum_q e_q^2 \frac{C_F}{2\pi}\frac{x^2}{Q^2}\int_{\mu^2/(1-x)}^{Q^2/x} d\ell^2 F_M(\ell^2)\alpha_s(\ell^2)\,.
\end{aligned}
\tag{4.12}
$$

In the case of the longitudinal structure function of the meson, we have eliminated the distribution amplitude ϕ in favor of the meson form factor (to leading order in α_s):

$$
F_M(\ell^2) = 16\pi C_F \frac{\alpha_s(\ell^2)}{\ell^2}\left[\int_0^1 \frac{dy}{1-y}\phi(y,\ell^2)\right]^2 \tag{4.13}
$$

where $\ell^2 \equiv \ell_\perp^2/(1-x)$.

The result (4.12) gives an absolutely normalized contribution $F_L^M \sim x^2\lambda^2/Q^2$ to the longitudinal meson structure function which will dominate the normal leading twist transverse contribution $F_1 \sim (1-x)^2$ at large x for fixed W^2.[35,36] In rough magnitude $\lambda^2 \simeq 0.1\ GeV^2$. It is interesting to note that in light-cone perturbation theory and $A^+ = 0$ gauge, the $x \to 1$ contribution to F_L^M is given entirely by an instantaneous fermion contribution [see Fig. 5(a)], i.e., an effectively local photon-gluon coupling. Since the instantaneous fermion does not radiate gluons, this contribution does not evolve to lower x in the standard way. In a sense the $Q^2 F_L^M$ contribution is similar to the point-like Born driving term in the photon-structure function,[37] although the operator mixing structure for F_L^M is evidentally more complicated.[38]

5. PHENOMENOLOGICAL CONSEQUENCES

The dominance of the higher twist longitudinal structure function of mesons in the endpoint region is a striking prediction of QCD. This result has implications[8] for a number of observable processes $MB \to \ell\bar{\ell}X$, $\ell B \to \ell' MX$, $e^+e^- \to MX$, and $H + H \to MX$. In each case the effective meson distribution or fragmentation functions have the form

$$G_{q/M}(x) \sim (1-x)^2 + \frac{\lambda^2}{Q^2} \tag{5.1}$$

and

$$D_{M/q}(z) \sim (1-z)^2 + \frac{\lambda^2}{Q^2} \tag{5.2}$$

where the $(1-x)^2$ and λ^2/Q^2 terms are associated with transverse and longitudinal currents, respectively. Evidence for dominance of the longitudinal current at large z has been reported in a Gargamelle analysis[39] of the quark fragmentation functions in $\nu p \to \pi^+ \mu^- X$. In e^+e^- annihilation the leading meson at $z \simeq 1$ should have a $sin^2\theta$ angular distribution relative to the beam direction.[40]

In the case of the Drell-Yan process the cross section has the angular form[8]

$$\frac{16\pi}{3} \frac{d\sigma}{dcos\theta d\phi} = \sigma_T(1 + cos^2\theta) + \sigma_L sin^2\theta + \sigma_{LT} cos\theta sin\theta cos\phi \tag{5.3}$$

where θ and ϕ specify the lepton direction in the virtual photon center-of-mass with the z-axis along the meson beam. With the definitions implied by (5.3), the total lepton pair cross section is $\sigma = \sigma_T + (1/2)\sigma_L$. In general, a fourth term is present in the angular distribution proportional to $sin^2\theta\, cos2\phi$. This term is not enhanced relative to σ_T by the high twist effect we investigate here. For large $x = x_1$, the contributions corresponding to Figs. 5(b) and 5(c) predict

$$\sigma_T \propto (1-x)^2 \ , \ \sigma_L \propto \frac{x^2\lambda^2}{Q^2} \tag{5.4}$$

with the normalization given in Eqs. (4.7), (4.11) and (4.12). Although σ_L can be absolutely normalized to the meson form factor, σ_T depends in detail on the shape of the distribution amplitude. If $\phi(y) \propto \delta(y - \frac{1}{2})$ (the weak binding approximation) then[8]

$$\frac{\sigma_L}{\sigma_T} = \frac{(4/9)x^2 \langle k_\perp^2 \rangle}{(1-x)^2 Q^2} \tag{5.5}$$

where $\langle k_\perp^2 \rangle$ is defined as the mean photon transverse momentum in $d\sigma_T/dk_\perp^2$ for $Mq \to \gamma^* q$. In general the longitudinal contribution should become visible when the measured meson structure function $G_{q/M}(x, Q)$ (or fragmentation function) becomes of the order of the predicted size of the higher twist contribution λ^2/Q^2 with $\lambda^2 = \mathcal{O}(0.1\, GeV^2)$.

The present data[41,42] for $\pi N \to \ell \bar{\ell} X$ are shown in Fig. 6 in terms of the parameter $\alpha = (\sigma_T - \sigma_L)/(\sigma_T + \sigma_L)$. A model prediction, assuming $\langle k_\perp^2 \rangle \sim 1\ GeV^2$ in Eq. (5.5) is also shown for comparison, although this is likely an overestimate of the QCD effect. The results from the two available measurements unfortunately disagree on the presence of a longitudinal component at large x_1. A third experiment, currently running at FNAL, should provide a definite test.

The interference contribution σ_{LT} gives additional sensitivity to the longitudinal current signaled by the $sin 2\theta\ cos\phi$ dependence. We find[8] from just the tree graphs $\sigma_{LT} = \sqrt{\sigma_L \sigma_T}$. However, as emphasized recently by Pire and Ralston[43] this contribution is sensitive to the phase ω between the longitudinal and transverse currents:

$$\sigma_{LT} = \sqrt{\sigma_L \sigma_T}\, cos\omega\, . \tag{5.6}$$

We also note that this $(1-z)/Q$ contribution should be observable in the $e^+e^- \to MX$ distribution at $z \to 1$ and moderate Q^2, and in $\ell N \to \ell' MX$.

We can also use the transverse momentum dependence of the virtual photon relative to the pion direction to further discriminate the leading and higher twist contributions. From Eqs. (4.7) and (4.13) we see

$$\frac{d\sigma_T}{dQ_\perp^2} \sim \frac{(1-x)^2}{Q_\perp^4} \; , \; \frac{d\sigma_L}{dQ_\perp^2} \sim \frac{x^2}{Q^2 Q_\perp^2} \; , \tag{5.7}$$

i.e., the higher twist longitudinal contribution has the same power-law fall-off in $Q_\perp$ as that obtained from gluon jet recoil. The absolutely normalized longitudinal subprocess cross sections for $\pi q \to \ell \bar{\ell} q$ (color averaged) in the kinematic region $Q_\perp^2 < Q^2$ is

$$\frac{1}{\pi} \frac{d\sigma_L(Mq \to \ell\ell q')}{d\hat{t}\, dQ^2\, dcos\theta} = \frac{8}{9} \cdot \frac{\alpha_s(\hat{t})\alpha^2 e_q^2}{Q^4} \cdot \frac{F_\pi(\hat{t})}{Q^2} \cdot \frac{sin^2\theta}{4\pi} \tag{5.8}$$

where $\hat{t} = (p_{q'} - p_\pi)^2 = -Q_\perp^2/(1-x_1)$. The transverse cross section depends, again, in detail on the form of the meson distribution amplitude:

$$\frac{d\sigma_T}{d\sigma_L} = \frac{(1-x_1)^2 Q^2}{4x_1^2 Q_\perp^2} |1 + r(x_1)|^2 \; . \tag{5.9}$$

Here

$$r(x_1) = \frac{\int_0^1 dy\, [\phi(y)/(1-y)][1/(x_1 - y + i\epsilon)]}{\int_0^1 dy\, [\phi(y)/(1-y)]} \tag{5.10}$$

where $\int_0^1 dy\, \phi(y) = (1/2\sqrt{n_c}) f_\pi$ is normalized to the pion decay constant. Note that the σ_T contribution contains an integral over a Glauber singularity from the initial state interaction diagrams [Fig. 5(c)]. There is also a corresponding contribution (at $Q_\perp = 0$) from the interference diagrams [Fig. 5(d)]. A more general analysis of such contributions including non-Abelian effects is given in Ref. 44.

Finally, we note that the F_L^M contribution is dependent on the valence wave function at small impact separation and is thus only sensitive to a relatively compact part of the meson wave function. Such small Fock components should have relatively negligible color interactions, suffering little effect from initial state induced radiation or transverse momentum smearing. As in the case of all the direct hadron-induced reactions discussed in this talk, there should be no associated central region multiplicity induced by collisions in the nuclear target.

ACKNOWLEDGEMENTS

We wish to thank M. Soldate, J. Gunion, P. Nason, and R. Blankenbecler for helpful conversations.

REFERENCES

1. For other reviews on higher twist/power-suppressed QCD contributions, see:

    (a) R. M. Barnett, Proceedings of the 1979 SLAC Summer Institute, p. 416 (1979).

    (b) E. L. Berger, Proceedings of the European Physical Society International Conference on High Energy Physics, Geneva (1979); Z. Phys. C4, 289 (1980).

    (c) S. J. Brodsky, G. P. Lepage, Proceedings of othe 20th International Conference on High Energy Physics, p. 805 (1980) and Proceedings of the SLAC Summer Institute (1979) (Prog. in Phys., Vol. 4, Brookhaven (1982)).

    (d) J. F. Gunion, Proceedings of the 3rd International Symposium on Elementary Particle Physics, Warsaw (1980).

    (e) R. Blankenbecler, Proceedings of the 15th Rencontre de Moriond, p. 463 (1980).

    (f) M. Moshe, Proceedings of the Advanced Summer Institute on High Energy Physics, Bad Honnef, Germany (1980).

    (g) H. D. Politzer, Proceeding of the Symposium on Topical Questions in QCD, Copenhagen, p. 934 (1980).

    (h) R. L. Jaffe, M. Soldate, Proceedings of the 1981 Conference of Perturbative QCD, Tallahassee (1981).

    (i) A. V. Radyushkin, Proceedings of Gauge Theories and Lepton-Hadron Interactions, p. 79 (1981).

2. N. Paver and D. Treleani, Nuovo Cimento A70, 215 (1982). H. D. Politzer, Nucl. Phys. B172, 349 (1980).

3. E. L. Berger and S. J. Brodsky, Phys. Rev. D24, 2428 (1981).

4. See R. L. Jaffe, M. Soldate, Phys. Rev. D26, 49 (1982), and references therein.

5. See, e.g., J. Ellis, M. K. Gaillard, W. Zakrewski, Phys. Lett. 81B, 224 (1979).

6. R. Blankenbecler and I. Schmidt, Phys. Rev. D16, 1318 (1977). L. Abbott, E. Berger, R. Blankenbecler and G. Kane, Phys. Lett. 88B, 157 (1979). L. Abbott and R. M. Barnett, Ann. Phys. (NY) 125, 276 (1980). R. M. Barnett and D. Schlatter, Phys. Lett. 112B, 475 (1982), and references therein. See also A. Donnachie, P. V. Landshoff, Phys. Lett. 95B, 437 (1980). R. L. Jaffe and M. Soldate, Phys. Lett. 105B, 467 (1981). B. P. Mahapatra, Phys. Rev. D25, 1 (1982). Heavy quark effects are discussed by R. M. Godpole and D. P. Roy, Z. Phys. C15, 39 (1982).

7. G. R. Farrar and D. R. Jackson, Phys. Rev. Lett. 35, 1416 (1975). A. I. Vainshtain and V. I. Zakharov, Phys. Lett. 72B, 368 (1978). Z. F. Ezawa, Nuovo Cimento 23A, 271 (1974).

8. E. L. Berger and S. J. Brodsky, Phys. Rev. Lett. 42, 940 (1979). E. L. Berger, Phys. Lett. 89B, 241 (1980). E. L. Berger, Ref. 1(b).

9. E. L. Berger, T. Gottschalk and D. Sivers, Phys. Rev. D23, 99 (1981).

10. For reviews and references, see R. Stroynowski in Prog. in Phys. Vol. 4, Birkhauser (1982), (Proceedings of the 1979 SLAC Summer Institute). S. J. Brodsky and G. P. Lepage, Ref. 1(c); and M. Jacob, EPS International Conference on High Energy Physics, Geneva, 1979, Vol. II, p. 473.

11. A more detailed paper is in preparation.

12. W. E. Caswell, R. R. Horgan, and S. J. Brodsky, Phys. Rev. D18, 2415 (1978).

13. R. K. Ellis, W. Furmanski, R. Petronzio, CERN-TH-3301 (1982). H. D. Politzer, Ref. 2. H. Georgi and H. D. Politzer, Phys. Rev. D14, 1829 (1976).

14. See, e.g., S. Gupta and H. Quinn, Phys. Rev. D26, 499 (1982).

15. S. D. Ellis, presented to the XIIIth International Symposium on Multiparticle Dynamics, Volendam (1982).

16. P. Renton and J. von Krogh, presented to the XIIIth International Symposium on Multiparticle Dynamics, Volendam (1982).

17. S. Gupta and H. R. Quinn, Phys. Rev. D25, 838 (1982).

18. G. P. Lepage and S. J. Brodsky, Phys. Rev. D22, 2157 (1980).

19. R. Blankenbecler and S. J. Brodsky, Phys. Rev. D10, 2973 (1974). S. J. Brodsky and G. Farrar, Phys. Rev. D11, 1309 (1975). S. J. Brodsky and G. P. Lepage, Ref. 1(c) (Appendix A).

20. J. A. Bagger and J. F. Gunion, Phys. Rev. D25, 2287 (1982). R. Rückl, S. J. Brodsky and J. F. Gunion, Phys. Rev. D18, 2469 (1978).

21. S. L. Grayson, M. P. Tuite, DAMTP preprint 81/27 (1982).

22. E. L. Berger, Phys. Rev. D26, 105 (1982). S. Matsuda, KEK-TH 37 (1981).

23. Such reactions were also the basis of the constituent interchange model for inclusive reactions. J. F. Gunion, S. J. Brodsky, and R. Blankenbecler, Phys. Rev. D8, 287 (1973). However, as shown by G. Fox and G. R. Farrar, Nucl. Phys. B167, 205 (1980); the p_T^{-8} reactions $\pi q \to \pi q$ have a small normalization in QCD.

24. For other tests of color transparency, see G. Bertsch, S. J. Brodsky, A. S. Goldhaber

and J. F. Gunion, Phys. Rev. Lett. 47, 297 (1981). A. Mueller, Proceedings of the 1982 Moriond Conference. S. J. Brodsky, SLAC-PUB-2970, and G. T. Bodwin, S. J. Brodsky, and G. P. Lepage, SLAC-PUB-2966, to be published in the Proceedings of the XIIIth International Symposium on Multiparticle Dynamics, Volendam (1982).

25. N. Isgur and M. Wise, Phys. Lett. 117B, 179 (1982).

26. E. L. Berger, S. J. Brodsky and G. P. Lepage (to be published). J. Hiller, private communication.

27. T. A. DeGrand, Y. J. Ng, and S.H.H. Tye, Phys. Rev. D16, 3251 (1977).

28. E. L. Berger, Ref. 1(b), and C. Peterson, D. Schlatter, I. Schmitt and P. Zerwas, SLAC-PUB-2912 (1982).

29. See, e.g., G. P. Lepage, S. J. Brodsky, T. Huang and P. B. Mackenzie, CLNS-82/522, to be published in the Proceedings of the Banff Summer Institute on Particle Physics (1982), and S. J. Brodsky, T. Huang, and G. P. Lepage, Proceedings of the 9th SLAC Summer Institute (1981).

30. S. J. Brodsky and G. P. Lepage, Ref. 1.

31. A. DeRujula and F. Martin, Phys. Rev. D22, 1787 (1980).

32. G. Baum et al., Phys. Rev. Lett. 45, 2000 (1980), and references therein.

33. E. G. Drukarev, E. M. Levin, V. A. Rozegauz, Leningrad preprint 764 (1982).

34. This result can also be obtained from light-cone perturbation theory. See S. J. Brodsky and G. P. Lepage, Proceedings of the 20th International Conference on High Energy Physics, p. 805 (1980). See also R. Blankenbecler, J. F. Gunion, and

P. Nason (to be published). A related result for fixed W^2 is given by A. Duncan and A. Mueller, Phys. Lett. 90B, 159 (1980).

35. For the operator product analysis of twist-4 contributions to the meson structure function at $x \to 1$, see M. Soldate, SLAC-PUB-2998 (1982).

36. The corresponding calculation of higher twist terms in the nucleon structure function is given by J. Gunion, P. Nason, and R. Blankenbecler, SLAC-PUB-2937 (1982). Large scale-breaking contributions are found. Note that Soldate (Ref. 35) and Gunion et al. include the power suppressed contributions to each structure function arising from the exact solution of the δ-function in Eq. (4.8).

37. E. Witten, Nucl. Phys. B120, 189 (1977). See also R. J. DeWitt et al., Phys. Rev. D19, 2046 (1979).

38. The operator analysis methods of Ref. 13 should be applicable to this problem.

39. M. Haguenauer et al., Phys. Lett. 100B, 185 (1981). C. Matteuzzi, APS DPF Annual Meeting, Santa Cruz, California (1981).

40. The data from the MARK I group at SPEAR do not show any indication of this effect at $Q^2 = 55 GeV^2$, $z \leq 0.9$. (J. Weiss, private communication.) Data at lower Q^2 would be very useful for this test.

41. K. J. Anderson et al., Phys. Rev. Lett. 43, 1219 (1979).

42. J. Badier et al., Z. Phys. C11, 195 (1981).

43. B. Pire and J. Ralson, this conference and ANL-HEP-CP-82-67.

44. G. Bodwin, S. J. Brodsky, and G. P. Lepage, SLAC-PUB-2927 (1982).

FIGURE CAPTIONS

1. Examples of higher twist dynamical processes (a) multiple scattering multijet production in pp collisions; and (b) interference $(e_a e_b)$ contribution to deep inelastic lepton-proton scattering.

2. Examples of multiparticle higher twist reactions. In each case the hard scattering subprocesses can be computed perturbatively. The light-cone wave functions $\psi(x_i, k_{\perp i})$ provide the required hadron distributions.

3. Examples of direct hadron higher twist reactions: (a) $\pi g \rightarrow q\bar{q}$, (b) $\pi q \rightarrow gq$, and (c) $q\bar{p} \rightarrow \bar{q}\bar{q}$. In each case the valence Fock state enters directly in the hard scattering subprocess.

4. (a) Direct high p_T meson production via $gq \rightarrow \pi q$. (b) Higher twist contribution to high p_T direct photon and lepton pairs via $\pi q \rightarrow \gamma^* q$. (c) and (d) Leading and higher twist contributions to the transverse momentum distribution of direct mesons relative to the quark jet in e^+e^- annihilation.

5. (a) Calculation of higher twist contribution to the pion structure functions at $x \rightarrow 1$. The vertical quark propagator in the last figure indicates instanteous fermion propagation in light-cone quantization. (b), (c) and (d): The corresponding contribution to lepton pair production $\pi p \rightarrow \ell\bar{\ell}X$ at large x_1. Diagram (c) contains an initial state Glauber contribution. Diagram (d) is the unitarity counter term to (c).

6. Data for the $(1 + \alpha cos^2\theta)$ distribution measured in $\pi^- N \rightarrow \ell\bar{\ell}X$ reactions as a function of the $\bar{q}$ momentum fraction x_1, where θ is the lepton angle relative to the pion beam in the $\gamma*$ cm. The CIP and NA3 data are from Refs. 41 and 42,

respectively. The dotted line is the higher twist prediction Eq. (5.5) with $\langle k_{\perp}^2 \rangle = 1\, GeV^2$.

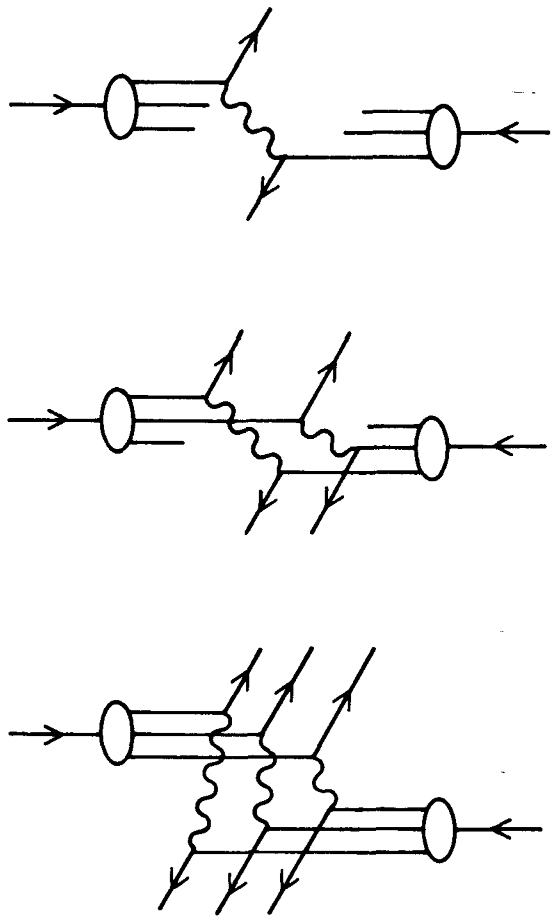

(a)

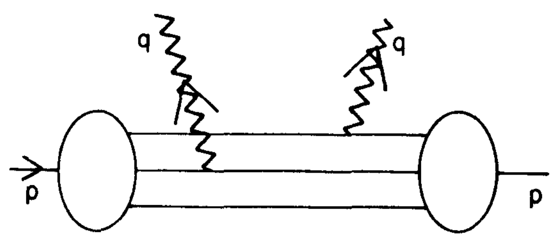

(b)

Fig. 1

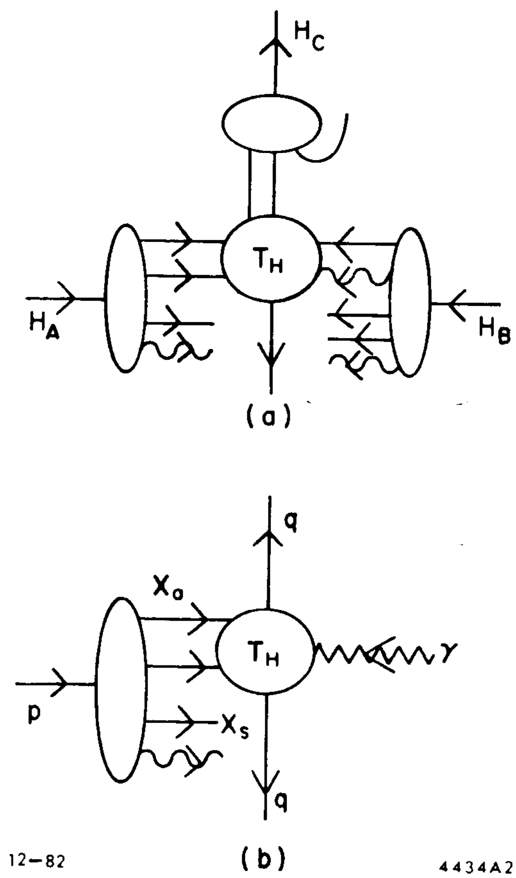

Fig. 2

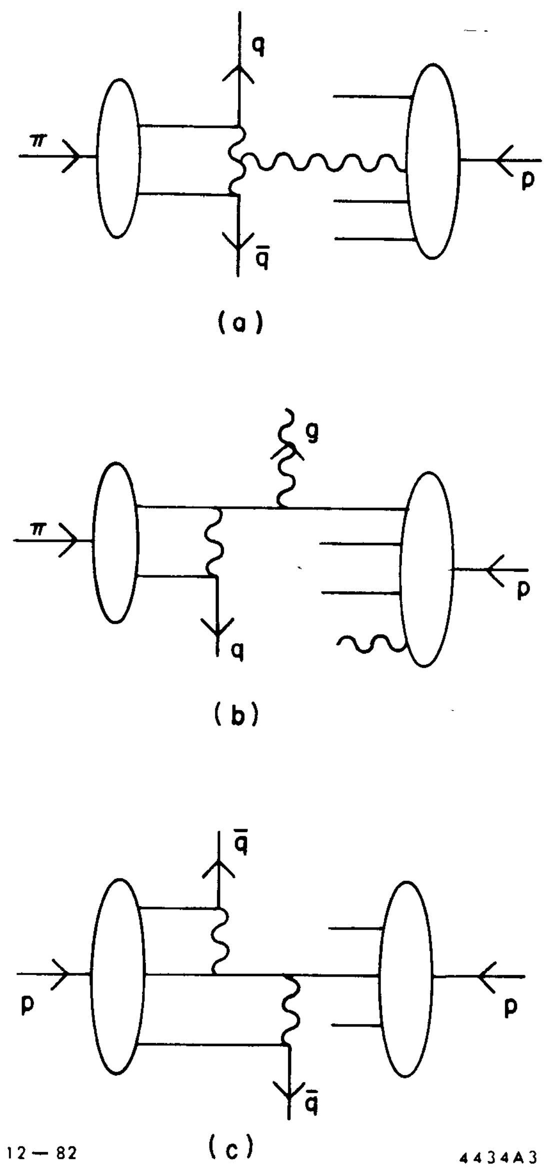

Fig. 3

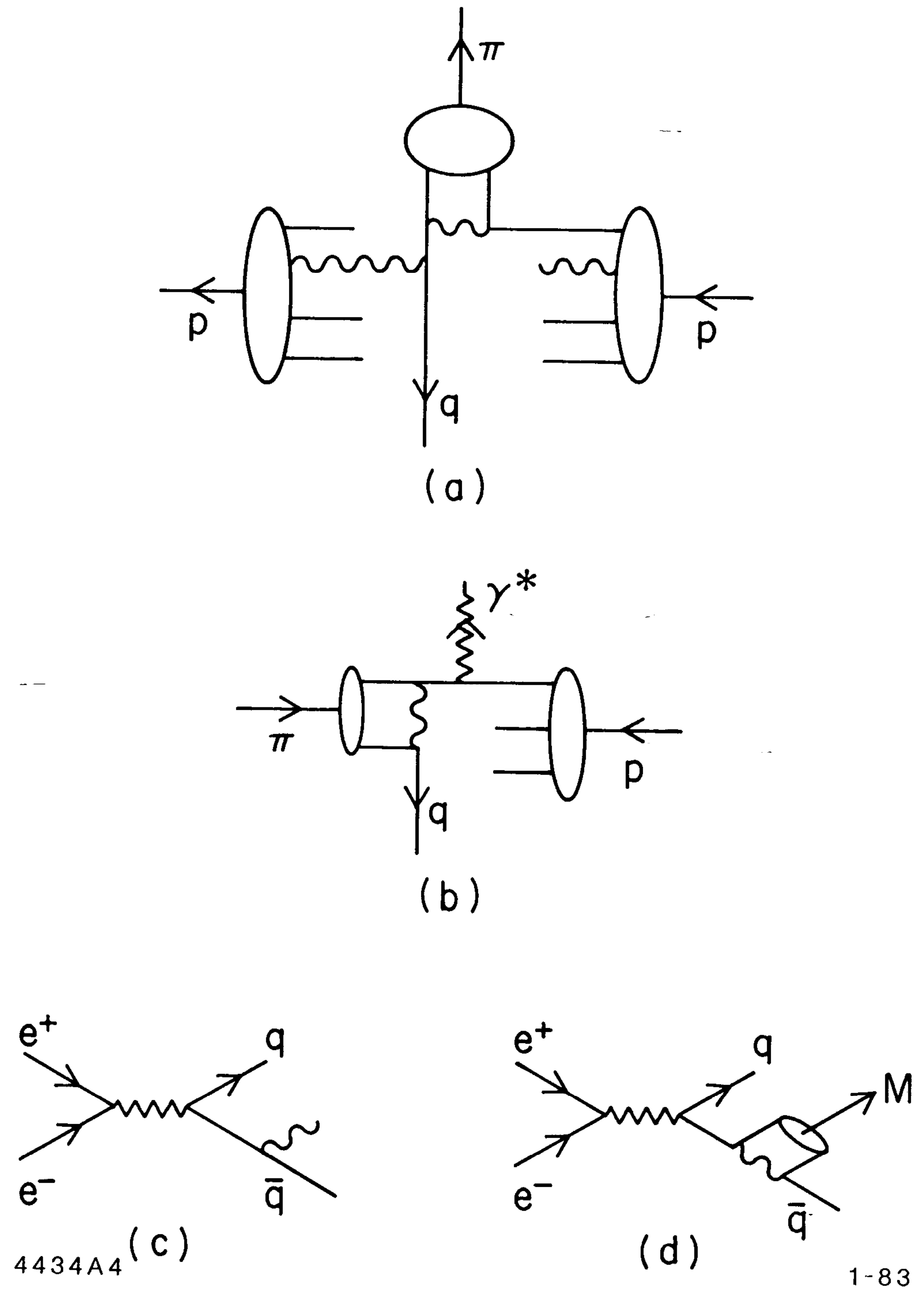

Fig. 4

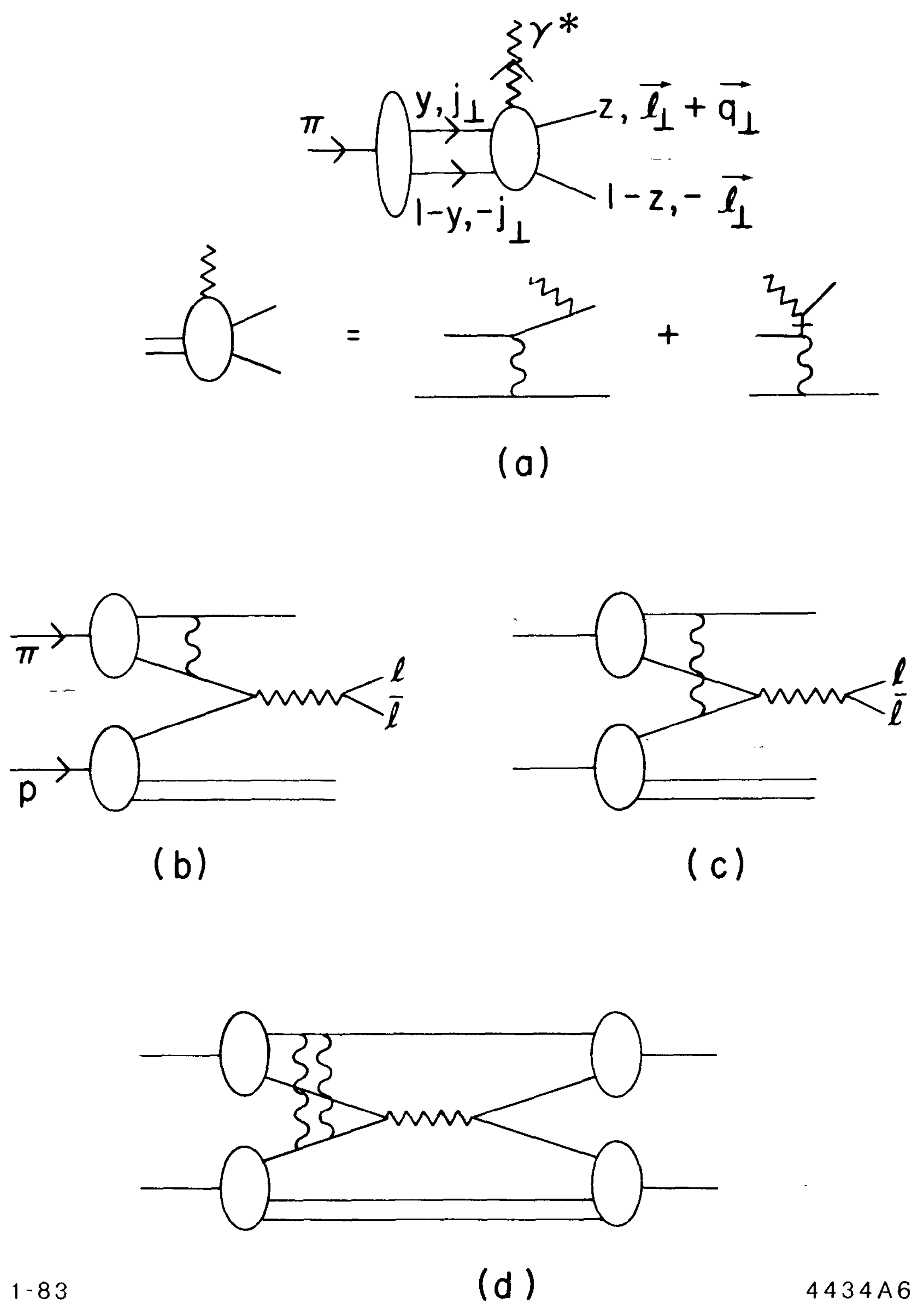

Fig. 5

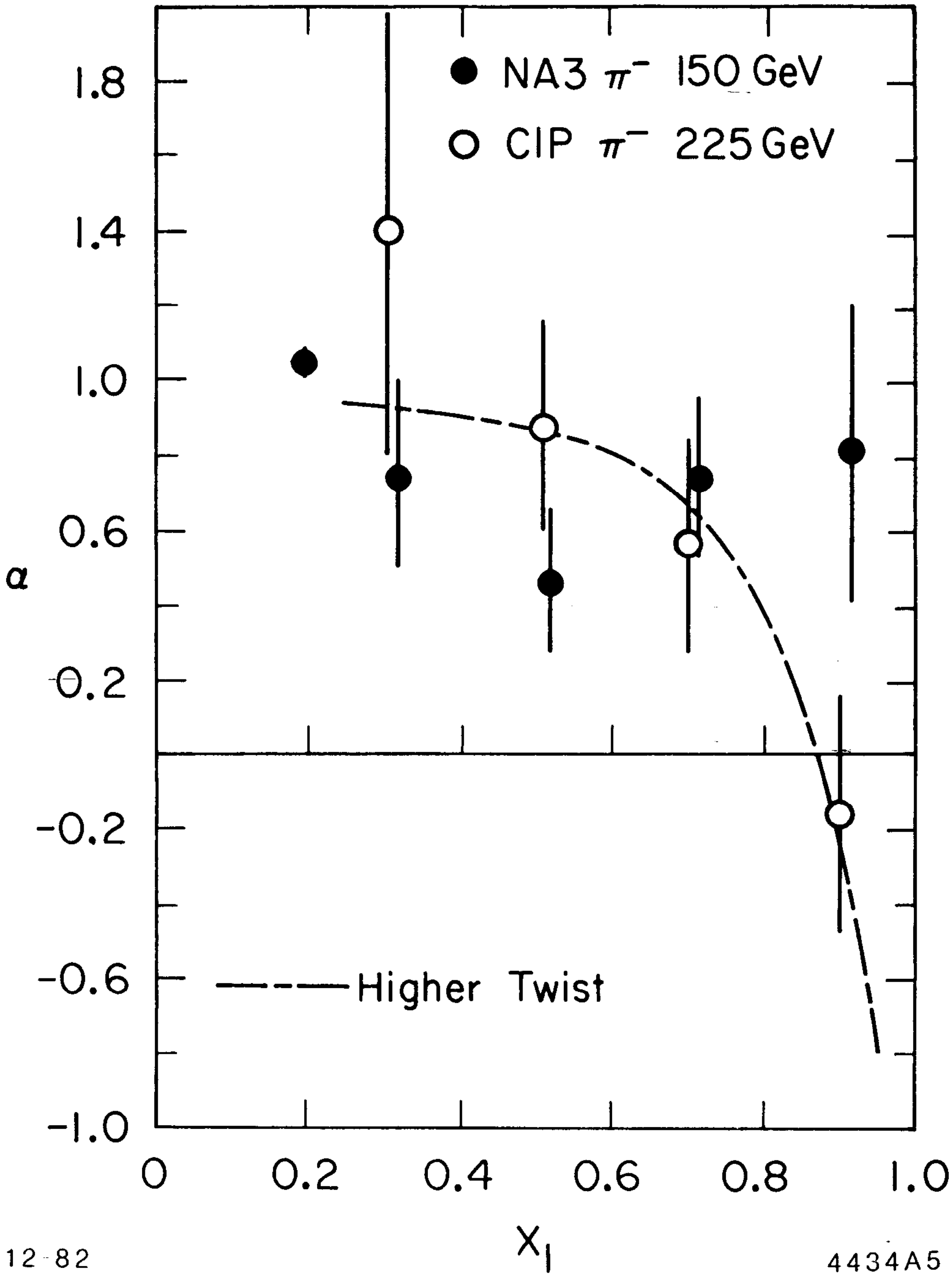

NA3 π⁻ 150 GeV
CIP π⁻ 225 GeV
1.8
1.4
1.0
0.6
0.2
-0.2
-0.6
-1.0
α
Higher Twist
0
0.2
0.4
0.6
0.8
1.0
X1
12-82
4434A5

Fig. 6